$LaNi_{5-x}Pt_x$: NMR investigation of structural and electronic properties

I. D. Weisman,* L. H. Bennett, and A. J. McAlister
Institute for Materials Research, National Bureau of Standards, Gaithersburg, Maryland 20760

R. E. Watson†
Brookhaven National Laboratory,‡ Upton, New York 11793
(Received 25 July 1974)

Pt-site Knight shifts κ, relaxation times, and crystallographic data have been obtained for the $LaNi_{5-x}Pt_x$ ($0 \leq x \leq 5$) system. There are two transition-metal sites: one, A, in a La layer and one, B, between La layers; different κ's are observed for each site. The system is found to be completely miscible and NMR intensities and crystallographic results show that Pt prefers the B site and that considerable ordering occurs for $x \lesssim 4$. The ^{195}Pt κ's are $\sim 1\%$ and $\sim 0\%$ for the A and B sites, respectively, in $LaPt_5$; the A-site κ is approximately 0 at $LaNi_4Pt$ and the B-site κ reaches -2% in $LaNi_{4.75}Pt_{0.25}$. The shifts, taken together with relaxation times, indicate that s-band effects dominate, particularly for the A site, in $LaPt_5$ and that the Pt atoms on both sites become more transition-metal-like with increasing x. Exchange enhancement is shown to be an essential factor at the Ni-rich end. Variations in chemical activity, as in hydride formation, are discussed in light of these electronic differences between $LaNi_5$ and $LaPt_5$.

I. INTRODUCTION

For technological as well as scientific reasons the rare-earth–transition-metal compounds having the $CaCu_5$ crystal structure have attracted considerable attention in the literature. $LaNi_5$ is one of the best metal mediums for the storage of hydrogen.[1] Along with such metals as titanium and vanadium, it absorbs a considerable amount of hydrogen per unit volume, but unlike these elements, it is remarkable in the ease of loading and of removal of the hydrogen from its matrix. While $LaPt_5$ is poorer[2] in its ability to absorb hydrogen, Pt is isoelectronic with Ni and has a spin-$\frac{1}{2}$-nucleus which is excellent as a nuclear-magnetic-resonance (NMR) probe. Furthermore, Pt and Ni metals are completely miscible, and it was decided to attempt to form and to study the $LaNi_{5-x}Pt_x$ alloy system. NMR-relaxation-time and Knight-shift results, taken with crystallographic data, are used to explore the electronic properties of this interesting system. The implication of these results to hydride formation is discussed in the final section.

$LaNi_5$, $LaPt_5$, and other rare-earth-Ni_5 compounds have the hexagonal structure displayed in Fig. 1. The RCo_5 (R being a rare earth) compounds also have this structure.[3,4] Their hydrogen absorption capacity is good, though inferior to that of their RNi_5 counterparts.[5] Their most prominent property is that they are strong ferromagnets, with the magnetism primarily associated with the Co_5 submatrix. For example, $SmCo_5$ has a high coercive force and a Curie temperature of 997 °K. While the Ni-rich end of Ni-Pt system is ferromagnetic, the $LaNi_{5-x}Pt_x$ system does not order magnetically, allowing conventional NMR studies. The RNi_5 compounds, with the rare-earth atoms having $4f$ moments, do display ferromagnetism[6] with $T_c < 30$ °K. This magnetic ordering is primarily associated with the rare-earth sites.

The RT_5 (T being a transition metal) compounds as a group are thus both chemically and magnetically active, and one approach to gaining insight into these properties is to study sequences with alloying at either the transition- or rare-earth-metal sites. Hydride formation[1,5,7] and other properties[6,8–11] have been studied as a function of alloying at either site. We are not aware of previous NMR studies for such alloy sequences. There have been no

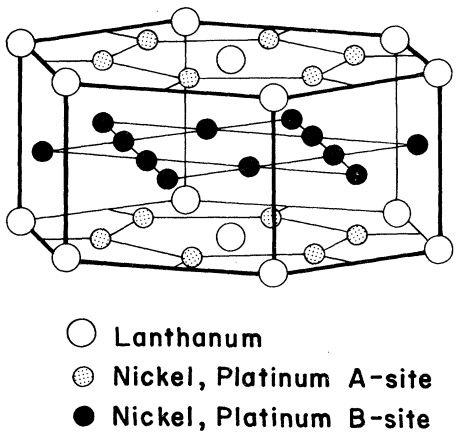

FIG. 1. Atomic arrangement in $LaNi_5$. This is the hexagonal $CaCu_5$-type structure [J. H. Wernick and S. Geller, Acta Crystallogr. 12, 662 (1959)], space group $P6/mmmm$. The atomic positions are La on $1a$, viz., (000), Ni^{I} on $2c$, viz., $(\frac{1}{3}, \frac{2}{3}, 0)$ and $(\frac{2}{3}, \frac{1}{3}, 0)$, here called A sites, and Ni^{II} on $3g$, viz., $(\frac{1}{2}, 0, \frac{1}{2})$, $(0, \frac{1}{2}, \frac{1}{2})$, and $(\frac{1}{2}, \frac{1}{2}, \frac{1}{2})$, here called B sites.

previous reports of any measurements on $LaNi_{5-x}Pt_x$ alloys, except for $LaNi_5$ and $LaPt_5$.

^{195}Pt Knight-shift results are reported in Sec. III A. Note that there are two crystallographically inequivalent transition-metal sites. The A sites, holding two of the five transition-metal atoms per molecular unit, lie in the basal plane with the rare earth. The B sites, holding the remaining three, lie between. Separate shifts are seen for Pt atoms on on the A and B sites. Monitoring the relative intensities in the two resonance lines provides a measure of the relative population of Pt at A and B sites, and it will be seen that $LaNi_2Pt_3$ shows considerable order with Ni at the A and Pt at the B sites. The Ni-Pt system also orders around certain, but different, critical concentrations. These tendencies toward order are expected in view of the difference in atomic sizes of Pt and Ni. Employing the Knight-shift κ and relaxation-time T_1 data, the κ will be partitioned into d and conduction or "s"-band components. Vijayaraghavan *et al.*[12] partitioned κ for $LaPt_5$, but, lacking the T_1 data obtained here, arrived at conclusions somewhat different from ours. In the extreme Ni-rich regime, the combined κ and T_1 data can be understood only if it is assumed that the alloy's Pauli susceptibility is exchange enhanced by a factor of 1.5 or greater. The question of exchange enhancement in a class of alloys which are chemically and magnetically active is, of course, of interest; unfortunately the NMR data do not allow any statements to be made concerning the variation in the enhancement across the alloy sequence.

While the NMR was used to make crystallographic statements, x-ray-diffraction results were obtained as well. These corroborate the ordering in $LaNi_2Pt_3$. The lattice parameters a and c are reported. The variation in a and c across the sequence are understandable, granted the tendency for Ni-Pt ordering. Although perhaps accidentally, the variation in a is strikingly like the variation in κ.

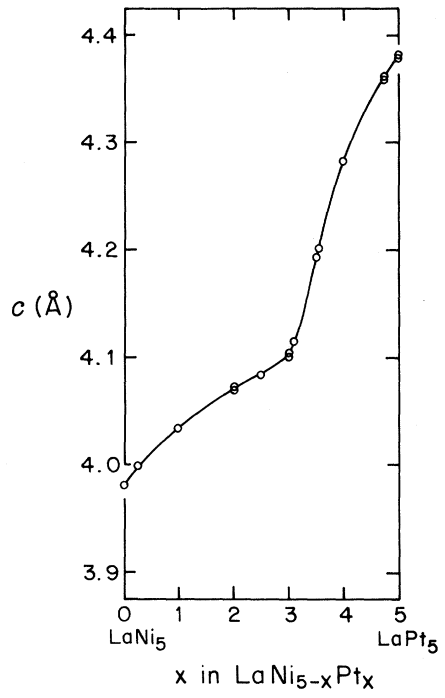

FIG. 2. Lattice parameter c vs Pt concentration for $LaNi_{5-x}Pt_x$, from x-ray diffraction measurements. The x values shown are nominal values except for the samples at $x=3.05$ and 3.54, which were prepared to nominal values of 3.00 and 3.50, respectively. They are shifted here and in subsequent figures by amounts determined from the c values of the other samples.

II. EXPERIMENTAL

A. Sample preparation

The $LaNi_{5-x}Pt_x$ compounds were prepared by arc melting on a water-cooled copper hearth with a nonconsumable tungsten electrode. The Ni and the Pt were fused first, and the alloy then melted with the La. About 2% excess La was used to compensate for losses by vaporization. Several inversions of the resulting buttons and remelting produced a homogeneous compound. The buttons were crushed using a mullite mortar and pestle, and sieved to -200 mesh.

The Ni-Pt composition of the compounds was determined by wet chemical analysis and by x-ray fluorescence. The root-mean-square deviation in x from the nominal compositions was found to be 0.1. Metallographic examination of the $LaNi_2Pt_3$ sample showed a single phase.

All the samples were examined by x-ray diffraction. These results confirm that there is complete solid solubility between $LaNi_5$ and $LaPt_5$, with evidence of ordering at $LaNi_2Pt_3$. The c and a crystallographic parameters are shown in Figs. 2 and 3 respectively, across the pseudobinary system $LaNi_{5-x}Pt_x$. Both parameters show approximately linear increases from $x=0$ (i.e., $LaNi_5$) to $x\approx 3$ (i.e., $LaNi_2Pt_3$). In this range of x, c expands less rapidly and a more rapidly than Vegard's rule predicts. Less obviously, linear variation asymptotically approaching Vegard's rule occurs near $x=5$ for both c and a.

The ratio c/a, obtained from the data of Figs. 2 and 3, is plotted in Fig. 4. In contrast to the relatively gentle changes seen for c and a, c/a displays a sharp deep minimum. At $x=3$, it has dropped to 0.772, a value markedly lower than the range generally observed[4] for RNi_5 compounds, which have c/a ranging from 0.793 for $LaNi_5$ to 0.822 for $CeNi_5$, hydrogen capacity[2] being higher for compounds of lower c/a. Similar behavior, though with less dependence of hydrogen absorption[5] on c/a,

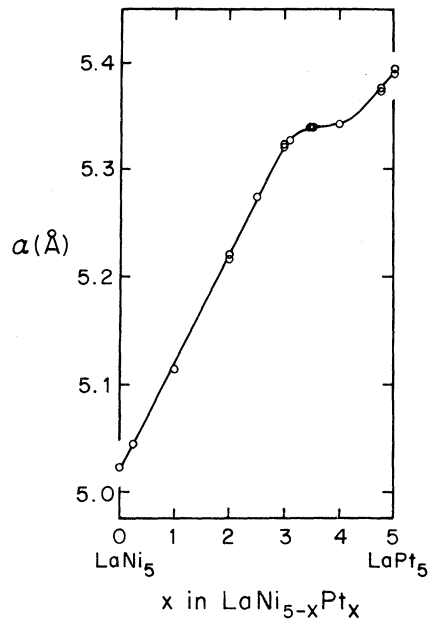

FIG. 3. Lattice parameter a vs Pt concentration for $LaNi_{5-x}Pt_x$, from x-ray diffraction measurements.

occurs for RCo_5 compounds, where c/a ranges[4] from 0.777 for $LaCo_5$ to 0.816 for $CeCo_5$. It would be of obvious interest to investigate the hydrogen absorption properties of $LaNi_{5-x}Pt_x$ alloys with c/a less than that of $LaNi_5$.

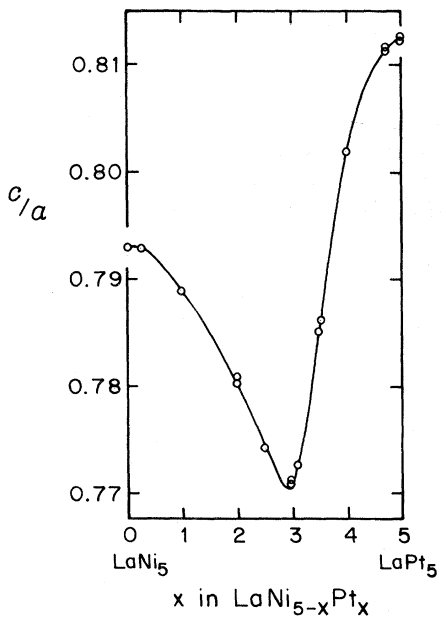

FIG. 4. Ratio of lattice parameters c/a vs Pt concentration for $LaNi_{5-x}Pt_x$.

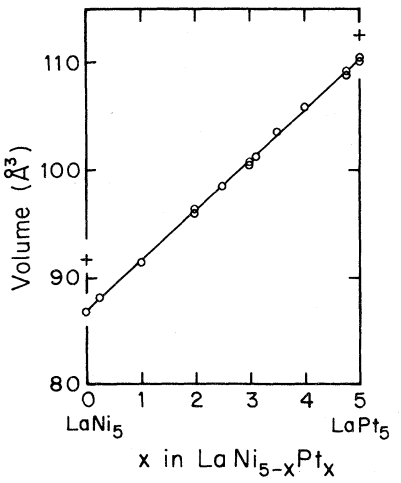

FIG. 5. Unit cell volume $\frac{1}{2}\sqrt{3}\,a^2c$ of $LaNi_{5-x}Pt_x$ as a function of x. Crosses at $x=0$ and 5 are the atomic volumes estimated from adding the individual atomic volumes (Ref. 13), respectively.

Interestingly, despite all the action in Figs. 3–5, the measured volume varies linearly throughout the alloy sequence, as seen in Fig. 5. The molar volumes for $LaNi_5$ and $LaPt_5$ are smaller than the sum of the atomic volumes,[13] the discrepancy being twice as large for $LaNi_5$ as for $LaPt_5$.

B. NMR equipment

All continuous-wave NMR data were taken with a commercial 2–16-MHz wide-line nuclear induction spectrometer, including signal averager and a 30-cm-pole-cap-diameter electromagnet. Low temperatures were achieved by immersing the sample in liquid nitrogen or liquid helium within a cold-finger-insert Dewar which fits into the NMR probes. All κ measurements were referenced to ^{195}Pt in iodoplatinic acid.

Pulsed NMR measurements were made with a phase-coherent and pulse-coherent crossed-coil spectrometer. The maximum rf field H_1 was 60 G at the lower frequency and 100 G at the higher frequency. Room-temperature measurements were made at 7.5 MHz using a 10-cm-pole-cap-diameter electromagnet. Liquid-helium-temperature measurements were made at 7.5 and 30 MHz using a superconducting solenoid with a 5-cm bore. A vacuum-dielectric gold-plated stainless-steel coaxial tube connected the transmitter and receiver cables to the probe assembly in the liquid-helium bath. At 30 MHz, some difficulty with rf heating of the samples was encountered. This problem was circumvented by resieving – 200 mesh powder through a 500 mesh screen and allowing the sample container to remain partially empty of powder. A sig-

nal averager, externally addressed by the pulse-sequence programmer, stored data points along the entire spin-lattice relaxation curve. Lineshapes obtained by integrating a spin echo with a boxcar integrator while sweeping the magnetic field were stored in the signal averager.

III. RESULTS AND DISCUSSION

A. cw results

The Knight shift κ of ^{195}Pt in $LaPt_5$ was measured at room temperature, 77 and 4.2 °K, and found to be slightly temperature dependent. The spectrum of the Pt resonance at room temperature, shown in Fig. 6, is in agreement with previous work.[12] Two distinct resonances are apparent, with intensity ratio 3:2 corresponding to the two crystallographically inequivalent sites. The separation between the two sites is 0.91% at room temperature and 1.00% at 4.2 °K.

Room-temperature Knight shifts of ^{195}Pt in $LaNi_{5-x}Pt_x$ ternary alloys were observed at both sites and are plotted versus x in Fig 7. The shifts of the A and B sites, to a good approximation, track each other over most of the range of x. The overall variation with x is reminiscent of the dependence of the lattice parameter a on x seen in Fig. 3. The negative Knight shifts in the Ni-rich region, like the shifts in many transition metals, are associated with the negative hyperfine field contributed by the d-band Pauli term. The magnitude of the temperature dependences in the alloys was similar to that observed in $LaPt_5$.

In general, the lines appeared to be symmetric with widths approximately proportional to the magnetic field. The cw linewidth (defined as the difference in field between the minimum and maximum slope of the absorption line), measured on the Pt B site at 14 MHz and room temperature, varied from 16(3) G in $LaPt_5$ to 61(12) G in the Ni-rich compounds. At 4 °K the widths were about twice as large. The absorption linewidths, as measured by the pulsed spectrometer, were broader by about a factor of 2 than would be inferred from integrating the corresponding cw line shapes (even under the assumption of a Lorentzian line). The pulsed method is probably distorting the observed lines, since its rf field H_1 is comparable to the true linewidths. Another possibility is that T_2, the spin-spin relaxation time, might be varying across the line and thus artificially flattening it. A comparison of T_2 at the resonance center and at the half-power point in the $LaNi_4Pt_1$ sample at 4.2 °K showed little variation; hence this explanation seems unlikely. Thus only cw relative-intensity and linewidth results are reported here.

The relatively strong symmetric broadening of the lines suggests that the linewidths are primarily

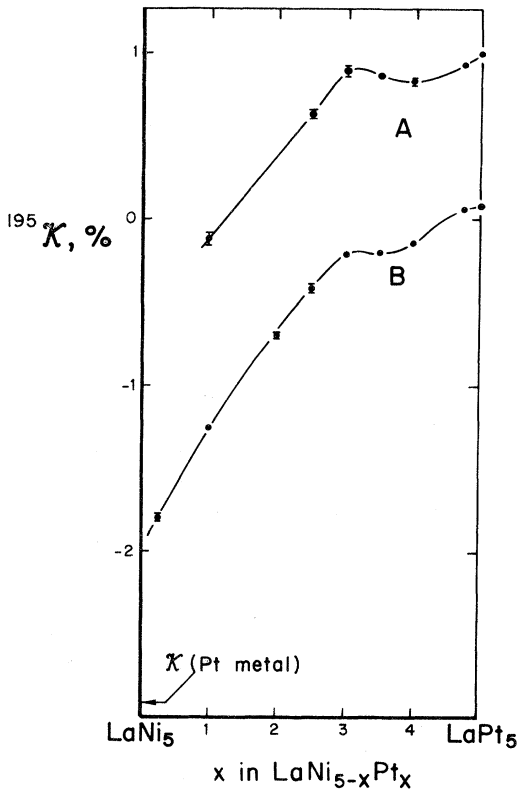

FIG. 7. Room-temperature Knight shift of ^{195}Pt in $LaNi_{5-x}Pt_x$ as a function of x. The upper curve is the shift at the A sites and the lower curve is the B-site shift. The $^{195}\kappa$ in Pt metal is indicated by the arrow. Error bars show the standard deviation in the mean. Where no bar is shown, the error is less than or equal to the dot diameter.

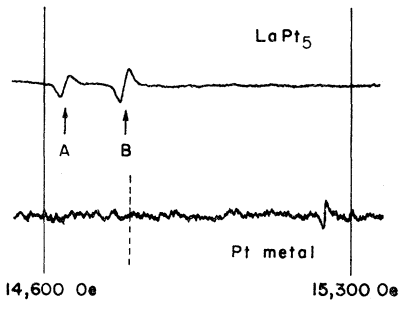

FIG. 6. Trace of the ^{195}Pt cw-absorption-derivative spectrum in $LaPt_5$ at room temperature and 13.5 MHz. The A- and B-site resonances are identified by arrows. In order to compare Knight shifts, the resonance of ^{195}Pt metal is shown in the lower trace on the same horizontal scale. Neither the vertical scale nor the number of scans for the two plots are the same. The vertical dashed line on the lower trace shows the position of the ^{195}Pt resonance in iodoplatinic acid.

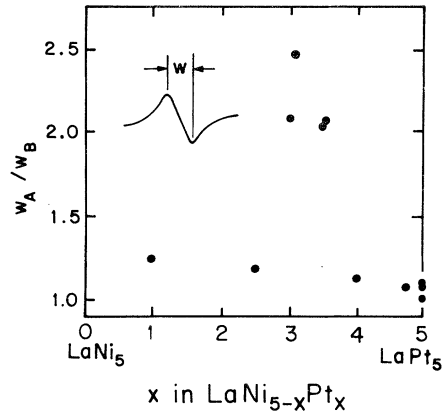

FIG. 8. Ratio of A-linewidth to B-linewidth ratio for ^{195}Pt resonance in $LaNi_{5-x}Pt_x$ vs x. The differences in width recorded at $LaPt_5$ may be due to measurement errors or stoichiometry variations.

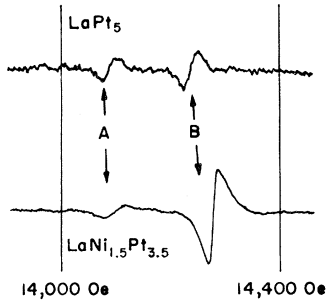

FIG. 10. Trace of the ^{195}Pt cw-absorption-derivative spectrum in $LaNi_{1.5}Pt_{3.5}$ plotted as a function of magnetic field (lower plot). For comparison of shifts, a trace of the ^{195}Pt spectrum in $LaPt_5$ is shown at the top of the figure. Both scans were taken at room temperature and 13.0 MHz. Neither the vertical scales nor the number of scans for the two plots are the same.

due to inhomogeneity of the Knight shifts arising from variations in local stoichiometry. Despite the noncubic symmetry, there is no measurable anisotropic Knight-shift contribution.

The ratios of the linewidths and of the peak-to-peak heights at Pt A and B sites at 14 MHz and room temperature are plotted in Figs. 8 and 9 as a function of x.

The ^{195}Pt spectrum of $LaNi_{1.5}Pt_{3.5}$ is compared with $LaPt_5$ in Fig. 10. The shift of the B site and the smaller shift of the A site (relative to the corresponding B and A sites of $LaPt_5$) can be seen. The A-to-B height ratio in the alloy is less than $\frac{2}{3}$ here. However, this is compensated by the width ratio, so that the integrated intensity ratio is near the random expectation, as is evident from Fig. 11. There is a sharp reduction of intensity at the A site in the $LaNi_2Pt_3$ alloy (not shown), which indicates that most of the Pt in this alloy resides at B sites. In other words, the NMR shows that there is a high degree of ordering of Ni on the A and of Pt on the B sites. X-ray crystallographic studies[14] support this observation.

The relative intensities (as measured by the product of the ^{195}Pt NMR amplitude and the square of the peak-to-peak width) of the A sites to B sites are used to deduce the fraction of A sites and of B sites occupied by Pt (see Fig. 11). The ordering at $LaNi_2Pt_3$, evident from Fig. 11, appears to be related to the plateau in the Knight-shift depen-

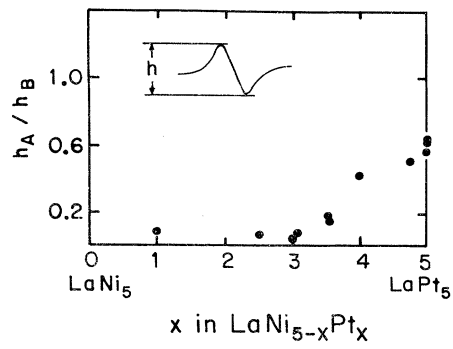

FIG. 9. Ratio of A height to B height for ^{195}Pt resonance in $LaNi_{5-x}Pt_x$ vs x.

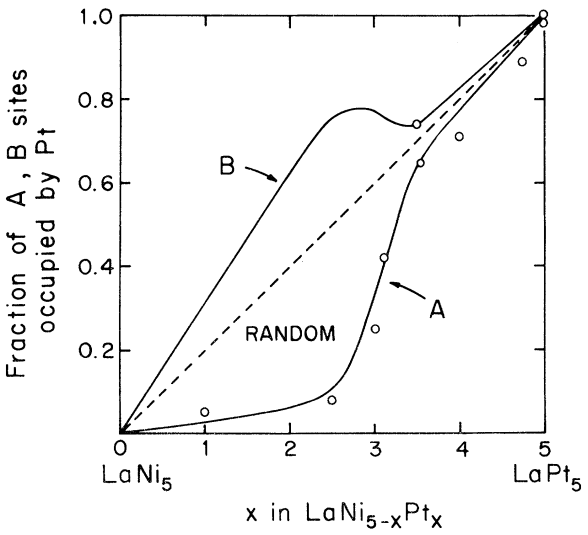

FIG. 11. Fraction of A and B sites occupied by Pt as determined from the NMR measurements. The dashed line is the random expectation. Points are A site fractions computed from the experimental width and amplitude ratios of Figs. 8 and 9. The solid A curve is drawn smoothly through the experimental points and the solid B curve computed from it.

dence shown in Fig. 7. Our results suggest that the NMR method may be more sensitive to changes in the A-site occupation in $LaNi_{5-x}Pt_x$ alloys than conventional x-ray methods. However, we have not attempted to determine the order-disorder transition temperature, if any, nor to control the heat treatment. At some values of x, measurements were made on two samples, nominally prepared in the same way (see caption to Fig. 2), with disparate results. The variations in ordering evident in Fig. 11, especially at $x \approx 3$, where the variation is outside experimental error, are likely to be due to small deviations in x from nominal values, or less probably, to inadvertent differences in heat treatment. Of course other factors, such as differences in La stoichiometry, may be at play.

The sharp peaking in the width ratio centered between $x = 3$ and 3.5 seen in Fig. 8 arises primarily from narrowing of the B site resonance, i.e., it would appear that B sites sample much less inhomogeneity in the Knight shift than do the A. Presumably this is associated in some way with the preferential site filling discussed in connection with Fig. 11. One can speculate on this; a $LaNi_{1.5}Pt_{3.5}$ structure can be visualized having a doubled unit cell where two-thirds of the B sublattice and three-quarters of the A are occupied by Pt atoms. In this structure all the B-layer Pt atoms have the same local environment while the A-layer Pt's encounter two distinctly different local environments. (These A sites have like nearest neighbors, implying a broadening rather than a splitting of the resonance line.) The peaking of the linewidth ratio to the right of $x = 3$ and the suggested bump in the A-site fraction of Pt occupancy (Fig. 11) at $x \sim 3.5$ are consistent with, while providing no proof of, such a second distinct Ni-Pt ordering. The present x-ray diffraction results do not help to resolve this speculation.

B. Spin-lattice relaxation

Spin-lattice relaxation was observed using either $\pi - t - (\frac{1}{2}\pi - \tau - \pi)$ or (saturation comb)$- t - (\frac{1}{2}\pi - \tau - \pi)$ pulse sequences, where $\tau = 30$ μs and where t could be varied incrementally in many steps over an interval that spanned three or four time constants.

The signal at each increment in t was stored sequentially in the memory of the signal averager, allowing sufficient time (8–10 T_1's) for the nuclear magnetization to equilibrate after each repetition. The entire spin-lattice relaxation curve was "scanned" in this fashion many times until a spin-lattice relaxation recovery curve with a reasonable signal-to-noise ratio could be observed in the memory. The comb consisted of from 1–40 pulses spaced 1 msec apart at 4.2 °K and 0.1 msec at room temperature. The pulse width was adjusted for maximum saturation. Although the condition $H_1 \gg W_{\mathrm{FWHM}}$ was not satisfied in most cases, the echo amplitude could be maximized with an approximate $\frac{1}{2}\pi - \pi$ sequence. No appreciable difference in relaxation was observed as a function of the number of pulses in the saturation comb.

For $LaPt_5$, the spin-lattice relaxation recovery curve appeared to consist of two exponential decays, each associated with one of the Pt sites. It was not possible to observe separately the relaxation from each site, although it was possible, by varying the magnetic field, to associate the slow component with the B site and the fast component with the A. The values of T_1 at these sites, listed in Table I, are quite different. The relaxation curves observed for $LaNi_{5-x}Pt_x$ ($x = 3, 2, 1, 0.25$) appeared to have only one exponential component, that associated with the Pt B site. The A-site resonance in these alloys is very weak or unobservable in both the cw and pulsed spectra. The values of T_1 on the Pt B site decrease with decreasing x.

C. Partitioning of Knight shifts

In principle, the experimental κ can be partitioned into components, the conduction electron contract term κ_s, the d-band core polarization term κ_{cp} and the Van Vleck orbital term κ_{orb}. Thus

$$\kappa = \kappa_s + \kappa_{cp} + \kappa_{orb}, \tag{1}$$

where usually κ_s and κ_{orb} are positive and κ_{cp} negative.

To estimate the terms of Eq. (1), use is made of a Korringa relation for hexagonal symmetry[15] and the experimental T_1,

$$\frac{1}{T_1 T} = A\left(\frac{\kappa_s^2}{\Gamma_s} + \frac{\alpha \kappa_{cp}^2}{\Gamma_{cp}} + \beta_{sd}\kappa_s\kappa_{cp}\right) + R_{orb}, \tag{2}$$

where $A = \pi k_B \hbar (\gamma_N/\mu_B)^2$; T is the absolute temperature, k_B the Boltzmann constant, γ_N the Pt nuclear gyromagnetic ratio, and μ_B the Bohr magneton. In Eq. (2), α is the orbital reduction factor which, for hexagonal symmetry, is expected to lie between 0.2 and 1. The Γ's are exchange-enhancement factors, and R_{orb} is the orbital contribution to spin-lattice relaxation. The weight, β_{sd}, of the cross term between the core polarization and the conduction-electron hyperfine terms is determined

TABLE I. Spin-lattice relaxation times at 4.2 °K.

Sample	Site	T_1 (msec)	$b = [\pi k_B \hbar (\gamma_N/\mu_B)^2 \kappa^2 T_1 T]^{-1}$
$LaPt_5$ [a]	A	11(4)	1.25
	B	42(3)	51.2
$LaNi_2Pt_3$	B	38.5(2.5)	8.94
$LaNi_3Pt_2$	B	33(2)	0.85
$LaNi_4Pt_1$ [a]	B	32(2)	0.28
$LaNi_{4.75}Pt_{0.25}$	B	30(4)	0.13

[a] T_1 was also measured at room temperature. T_1T was approximately the same as at 4.2 °K.

by such factors as the symmetry of the lattice and, in turn, by how many of the d bands intersecting the Fermi level hybridize to the s band.[15] It is expected that β is less than α, more of the order of 0.1 than 1.

There are too many variables to permit an unambiguous partitioning of κ. As a first approximation, neglect the s-d mixing term, the orbital terms $R_{\rm orb}$ and $\kappa_{\rm orb}$, and the exchange enhancement (i.e., set $\Gamma_s = \Gamma_{\rm cp} = 1$). Employing the useful combination of experimental parameters, $b = (A\kappa^2 T_1 T)^{-1}$, Eqs. (1) and (2) can then be solved for

$$\kappa_s = \kappa[\alpha/(1+\alpha)]\{1 \pm [1-(1+\alpha)\,(\alpha-b)/\alpha^2]^{1/2}\}. \quad (3)$$

Values of b are shown in Table I. A real solution to Eq. (3) requires that $\alpha \leq b/(1-b)$. Moreover, when κ is negative (as it is at the B site when $x \leq 4$), the observation that κ_s is always positive demands the more stringent condition

$$\alpha \leq b. \quad (4)$$

As already discussed, the minimum value of α is 0.2. Thus Eq. (4) is violated and no solution of Eq. (3) is possible for $x = 0.25$, the alloy for which $b = 0.13$ (see Table I). Hence at least one of the simplifying assumptions leading to Eq. 3 must be relaxed. Turning on the s-d mixing terms tends to overcome the restraint imposed by Eq. (4), but a $\beta_{sd} \sim 0.6$ is required to obtain a real solution of κ_s for $x = 0.25$. Such a value of β_{sd} appears to be unrealistically high.

Inclusion of exchange-enhancement factors of $\Gamma_s = 1$ and $\Gamma_{\rm cp} > 1.54$ will allow a real solution at $x = 0.25$. Such values are not unreasonable for transition metals with $A\kappa^2 T_1 T$ in the range encountered here.[16-18] If the orbital terms $R_{\rm orb}$ and $\kappa_{\rm orb}$ are included without exchange enhancement, using values appropriate[16,17] to Pt metal ($R_{\rm orb} \approx 47.5$ sec^{-1} °K^{-1}, $\kappa_{\rm orb} \approx 0.5\%$), no real solutions for κ_s at the B site can be obtained for any value of x. Scaling the orbital terms down to allow real solutions for κ_s requires invoking exchange enhancement up to higher values of x. Exchange enhancement is plausible in this alloy system and the present experiments provide evidence for its presence. It is now useful to inspect the values of κ_s and $\kappa_{\rm cp}$ obtained with varying values of $\Gamma_{\rm cp}$, as is done in Figs. 12 and 13. In these plots, it is assumed that $R_{\rm orb} = \kappa_{\rm orb} = \beta_{sd} = 0$, $\alpha = 0.2$, and in Fig. 13 $\Gamma_s = 1.0$. Note that the B results are displayed as curves of contant $\Gamma_{\rm cp}$ for convenience only, since $\Gamma_{\rm cp}$ need not be constant across the system. In fact, since $LaPt_5$ is diamagnetic[9] and $LaNi_5$ paramagnetic,[8] we would expect considerable variation in $\Gamma_{\rm cp}$. It is of interest to note that, if $\Gamma_{\rm cp}$ reaches some large value (~ 5–10) near $x = 0$, κ_s may be approximately constant across the system. Γ_s is expected to be less than $\Gamma_{\rm cp}$, unless such factors as s-d hybridization in the bands force it to approach $\Gamma_{\rm cp}$ in magnitude. The effect of choosing Γ_s greater than 1 involves, as is noted on the ordinate of Fig. 12, a simple scaling of the κ_s. Along with this scaling, there is a compensating shift of the $\kappa_{\rm cp}$ of Fig. 13. Neither this nor the presence of nonzero orbital terms qualitatively affects the conclusions concerning exchange enhancement.

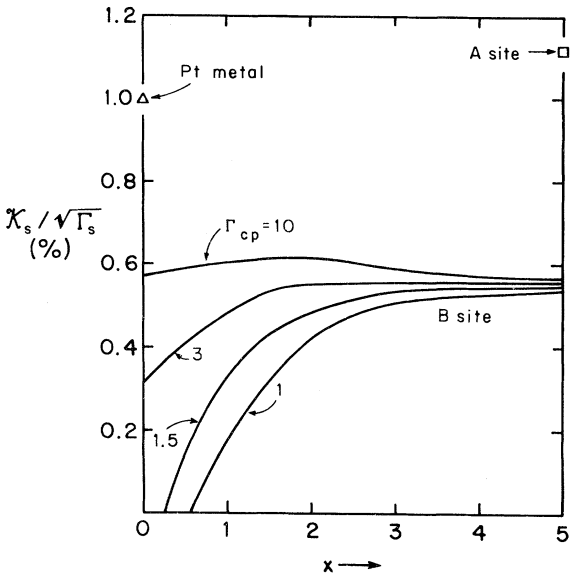

FIG. 12. Estimates of the direct-contact Knight shift divided by $\sqrt{\Gamma_s}$ obtained from Eq. (5) for various values of the core-polarization exchange-enhancement factor $\Gamma_{\rm cp}$. The assumptions affecting these estimates are described in the text. Partitioning at the A site is limited to $x = 5$, the only value of x at which A-site T_1 data was obtained. The variation of the A-site κ_s at $x = 5$ with $\Gamma_{\rm cp}$ was negligible. The value of κ_s for Pt metal (Ref. 17) is also shown.

IV. OBSERVATION AND CONCLUSIONS

Before concluding, let us make some observations concerning the tendency to hydride formation as well as the catalytic and electrode behavior of these alloys. While for the RT_5 compounds in general there are hints of correlations between the number of hydrogen atoms $n_{\rm H}$ absorbed per alloy molecule and the lattice parameters, the relationship is not simple. It is generally accepted that there is a minimum distance between hydrogen interstitial sites which is required if compound formation is to be achieved; apparently the RT_5 compounds considered in this paper meet this criterion. There is no simple dependence on volume factors. For example, not only is the molecular volume of $LaPt_5$ larger than that of $LaNi_5$, but, more importantly, one expects that the volume available to H_2

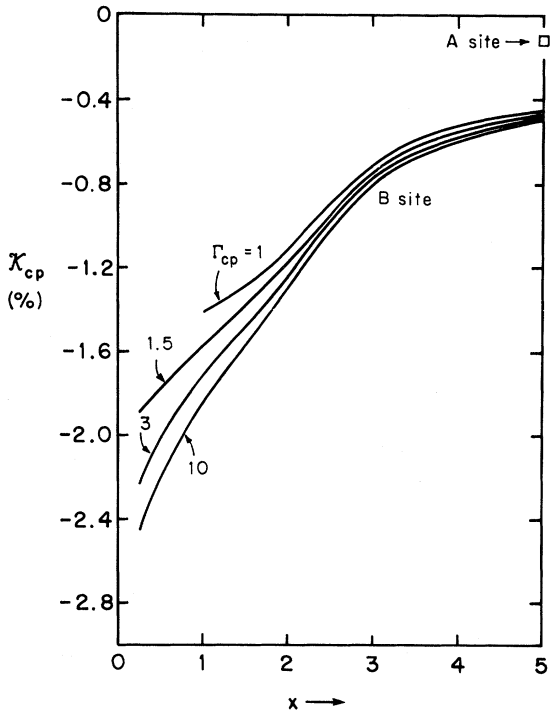

FIG. 13. Estimates of the d-band core-polarization contribution to the Knight shift obtained from Eq. (3) for various values of Γ_{cp}, under assumptions identical to those for Fig. 12. The value of κ_{cp} for Pt metal falls off the scale of the figure near -4.5%.

storage is greater in the former, as was noted in Fig. 5; the molecular volumes of the compounds are smaller than the appropriate sums of Ni, Pt, and La metallic volumes and this compression is greater in the Ni compound. Despite this, $LaNi_5$ absorbs more hydrogen. A compression occurs on formation of any of the RT_5 compounds, and, while there are correlations within classes of compounds (e.g., n_H increases with decreasing compression or decreasing c/a in either the RNi_5 or RCo_5 sequence, but decreases, when these factors decrease, on going from a given RNi_5 to its Co_5 or Pt_5 counterpart), there is no overall relation between compression and hydrogen-absorption capacity. Still more important would be a comparison between hydrogen-absorption capacity and the increase in molecular volume associated with the addition of H to the lattice. This comparison is hampered by little data; none, of which we are aware, exists for adding H to the $LaPt_5$ system. For fcc metals and alloys, a striking correlation exists[19] between the volume increase and the hydrogen content. The RT_5 data available[5] do not fall on the same curve.

While some volume restrictions must necessarily be met if hydride formation is to occur, such volume factors are not sufficient to determine the propensity for accepting hydrogen. The electronic structure properties of the host metals are clearly of importance. The present NMR results indicate that $LaNi_5$ is more transition-metal-like than $LaPt_5$, implying[20] greater chemical activity involving hydrogen. The NMR also show stronger exchange enhancement, which we believe is a concomitant of hydrogen activity. The connection between such manifestations of electronic structure and hydride formation is, at this stage, only qualitative in nature, but there do exist several quantitative models which should be considered. For example, in discussion of the fcc metals, Switendick[21] has correlated the propensity for dilute H_2 solution with the presence of one-electron states above E_F in the pure metal which have s-like character with respect to the hydrogen interstitial sites. In another approach Van Mal, Buschow, and Miedema[22] have applied Miedema's model[23] of the heat of alloy formation to the problem of H absorption in the RT_5 compounds. For a binary alloy, the heat of formation per atom is taken to be

$$\Delta H = f(c)\,[-P(\Delta\phi)^2 + Q(\Delta N_w)^2], \tag{5}$$

where $f(c)$ is a concentration-dependent factor, P and Q are constants, $\Delta\phi$ is the difference in chemical potential, and Δn_w is the difference in electron density at the Wigner-Seitz sphere radius, between the separate constituent metals. The ϕ have been deduced using work-function data (i.e., an unwanted metal-surface dipole term is present), and the scheme has been extraordinarily successful in correlating the heats of formation of binary alloys. Van Mal *et al.* extended this to the RT_5H_x case; calculations for $LaNi_5$ and $LaCo_5$ yielded a ΔH which indicated that H_6 was preferable to H_4 in the Ni compound and the reverse for Co, as is indicated in Table II. We have done equivalent calculations for $LaPt_5$, with the results (see Table II) indicating that an n_H of 6 is to be preferred, and,

TABLE II. Heats of reaction for various RT_5H_x systems as calculated by Van Mal *et al.* (Ref. 22) for $LaNi_5H_x$ and $LaCo_5H_x$, and calculated in the same way here for $LaPt_5H_x$.

	ΔH (kcal/mole H_2)
$LaNi_5H_6$	-6.5
$LaNi_5H_4$	-4.5
$LaPt_5H_6$	-4
$LaPt_5H_4$	-1
$LaCo_5H_6$	-11.8
$LaCo_5H_4$	-13.5

if it is assumed that the magnitude of ΔH correlates with the pressure, then $LaPt_5$ should accept hydrogen at roughly the same pressure as $LaNi_5$. Both predictions are contrary to fact.[2] Volume corrections to the heats of reaction and neglected entropy may account for this discrepancy, although the problem may be more fundamental; chemical activity of the sort suggested by a strong exchange-enhanced susceptibility is absent from the model.

Concerning catalysis, it has been noted that a number of hydrogenation reactions show increased rates relative to the rate over pure Ni when catalyzed over H-charged $LaNi_5$.[5] (Since La is very sensitive to oxygen, the surface layer was observed to be depleted of La and the catalytic activity here was ascribed to pure Ni.) It is of obvious interest to investigate the catalytic activity over the full range of the pseudobinary $LaNi_{5-x}Pt_x$ system. In addition, some insight as to the importance of the electronic factor in catalysis should be provided by studies of the modification of the catalytic activity of Pt when incorporated into $LaPt_5$ (assuming of course, that La surface depletion can be excluded in the experiments).

Recently, $LaNi_5$ has proved to be a useful hydrogen-storage material for closed nickel/hydrogen batteries for aerospace applications.[24] A separate Pt-hydrogen-oxidation electrode has to be supplied in this case. In view of the Pt-metal-like properties of dilute Pt in $LaNi_5$ observed here, it is interesting to speculate whether the Pt electrode could be replaced in this system by dilute alloy additions of Pt to $LaNi_5$. Of course, it is important that the Pt does not severely poison the hydrogen-storage capabilities of the $LaNi_5$ if a common electrode and storage medium is to be achieved.

The above-mentioned properties provided one motivation for studying the $LaNi_{5-x}Pt_x$ system. The investigation indicates strikingly different electronic properties at the two ends of the row. The measurement of relaxation times in conjuction with the Knight shifts has enabled us to assess the importance of various contributions to the Knight shift across the series. The earlier suggestion[12] that in $LaPt_5$ the s term in the Knight shift is the same at both A and B sites, with the core polarization term zero at the A, is definitely ruled out by the present work. Distinct s- and core-polarization terms are present at both sites in $LaPt_5$. Upon addition of Ni, there is a marked increase in the core-polarization contribution. The strongly negative A- and B-site shifts observed at high Ni concentration have been shown to be the result of strong exchange enhancement typical of a transition metal. The behavior of $LaPt_5$ is not typical of a transition metal. Exchange enhancement is expected to be a concomitant of strong chemical activity.

In addition, continuous solid solubility is observed across the series. Considerable ordering occurs between $LaNi_5$ and $LaNi_{1.5}Pt_{3.5}$. While transition-metal-site ordering has been observed before[9-11] in alloys of this structure, the ordering seen here is the strongest yet reported; at $LaNi_2Pt_3$ it approaches compound formation of a new structural type. Less certainly, another type of ordering may be occurring at $LaNi_{1.5}Pt_{3.5}$. These properties make the $LaNi_{5-x}Pt_x$ system a promising system for studies of chemical activity.[25]

ACKNOWLEDGMENTS

We are grateful to D. P. Fickle for preparation of the alloys used in this investigation, to C. J. Bechtoldt for providing the extensive x-ray data reported here, and to R. K. Bell and R. L. Myklebust for the x-ray fluorescence measurements. R. L. Parke provided important technical aid with the measurements.

---

*Present address: Ph. D.-M. D. Program, University of Miami, Miami, Fla. .

†Also a consultant with the National Bureau of Standards.

‡Work supported by the U.S. Atomic Energy Commission.

[1]J. H. N. van Vucht, F. A. Kuijpers, and H. C. A. M. Bruning, Philips Res. Rep. 25, 133 (1970).

[2]J. L. Anderson, T. C. Wallace, A. L. Bowman, C. L. Radosevich, and M. L. Courtney (unpublished).

[3]E. A. Nesbitt and J. H. Wernick, *Rare Earth Permanent Magnets* (Academic, New York, 1973).

[4]K. N. R. Taylor, Adv. Phys. 20, 551 (1971).

[5]F. A. Kuijpers, Philips Res. Rep. Suppl. 28, 1 (1973).

[6]E. A. Nesbitt, H. J. Williams, J. H. Wernick, and R. C. Sherwood, J. Appl. Phys. 33, 1674 (1962).

[7]R. H. Wiswall and J. J. Reilly, in *Proceedings of the Seventh Intersociety Energy Conversion Engineering Conference, San Diego* (American Chemical Society, Washington, D.C., 1972), p. 1342.

[8]W. E. Wallace, *Rare Earth Intermetallics* (Academic, New York, 1973).

[9]K. S. V. L. Narasimhan, V. U. S. Rao, and R. A. Butera, AIP Conf. Proc. 18, 1081 (1972); A. M. Van Diepen, K. H. J. Buschow, and J. S. van Wieringen, J. Appl. Phys. 43, 645 (1972).

[10]M. Atoji, I. Atoji, C. Do-Dinh, and W. E. Wallace, J. Appl. Phys. 44, 5096 (1973).

[11]J. LaForest and J. S. Shah, IEEE Trans. Magn. MAG-9, 217 (1973).

[12]R. Vijayaraghavan, S. K. Malik, and V. U. S. Rao, Phys. Rev. Lett. 20, 106 (1968).

[13]W. B. Pearson, *The Crystal Chemistry and Physics of Metals and Alloys* (Wiley, New York, 1972).

[14]C. Bechtoldt (private communication) reports that an ingot having nominal composition $LaNi_2Pt_3$ shattered when struck gently into many small platelets. The cleavage face was found by Laue back reflection to be

the (0001) face. Precession patterns made about the *c* axis and *hho* axis (zero level) gave spots whose intensities were consistent only with the preferential filling of Pt atoms in *B* sites.

[15]A. Narath, Phys. Rev. 162, 320 (1967).

[16]Y. Yafet and V. Jaccarino, Phys. Rev. 133, A1630 (1964).

[17]A. M. Clogston, V. Jaccarino, and Y. Yafet, Phys. Rev. 134, A650 (1964).

[18]J. Butterworth, Phys. Rev. Lett. 8, 423 (1962).

[19]B. Baranowski, S. Majchrzak, and T. B. Flanagan, J. Phys. F 1, 258 (1971).

[20]See, for example, E. L. Muetterties, *Transition Metal Hydrides* (Marcel Dekker, New York, 1971).

[21]A. C. Switendick, in *The Hydrogen Economy Miami Energy (THEME) Conference* paper S6-1. (University of Miami, Coral Gables, Fla., 1974).

[22]H. H. Van Mal, K. H. J. Buschow, and A. R. Miedema, J. Less-Common Metals 35, 65 (1974).

[23]See, for example, A. R. Miedema, J. Less-Common Metals 32, 117 (1973).

[24]M. W. Earl and J. D. Dunlop, COMSAT Technical Review 3, 437 (1973); M. W. Earl and J. D. Dunlop, in Proceedings of the 26th Power Sources Symposium, Atlantic City, N. J., 1974, (to be published).

[25]The hydrogen-absorption capability of $LaNi_{5-x}Pt_x$ is currently being investigated by R. H. Wiswall and J. J. Reilly.